Available online at www.sciencedirect.com

ScienceDirect

Ceramics International 40 (2014) 3145–3148

CERAMICS INTERNATIONAL

www.elsevier.com/locate/ceramint

One step solid state synthesis of $FeF_3 \cdot 0.33H_2O$/C nano-composite as cathode material for lithium-ion batteries

Xiaoping Xu, Shu Chen, Miao Shui*, Lingxia Xu, Weidong Zheng, Jie Shu, Liangliang Cheng, Lin Feng, Yuanlong Ren

The State Key Laboratory base of Novel Functional Materials and Preparation science; The Faculty of Materials Science and Chemical Engineering, Ningbo University, Ningbo 315211, PR China

Received 6 September 2013; received in revised form 12 September 2013; accepted 27 September 2013
Available online 8 October 2013

Abstract

Nanometer-sized $FeF_3 \cdot 0.33H_2O$/acetylene black composite has been synthesized by one step chemico-mechanical ball-milling process using Fe $(NO_3)_3$•$9H_2O$ and NH_4F as precursors and investigated as cathode materials for secondary lithium batteries. The obtained $FeF_3 \cdot 0.33H_2O$/C composite was described in terms of structure, morphology, and electro-chemical performance. The composite exhibited a noticeable capacity of 233.9 mAh g^{-1} at a current density of 20 mA g^{-1} within potential range 1.8–4.5 V and good rate capability. These results showed that $FeF_3 \cdot 0.33H_2O$/C nano-composite prepared from an easily scalable chemico-mechanical ball-milling process was of great industrial interest.

Keywords: Nanocomposites; Li-ion battery; Iron fluoride; Chemico-mechanical ball-milling

1. Introduction

In recent years, transition metal fluorides have drawn considerable attention due to their high theoretical energy density and high operating voltage as cathode materials for LIB. Unlike typical lithiated transition metal oxides ($LiMO_2$, M=Co, Ni, and Mn), these materials, based on Li-driven conversion reaction, can produce a large multi-electron redox capacity. Among these metal fluorides, iron-based fluorides are of great attraction in terms of their low cost and low toxicity. Furthermore, FeF_3 has high theoretical capacity (712 mAh g^{-1}, 3 electrons transfer) and good thermal stability [1]. However, the high electro-negativity of fluorine induces a large bond gap, and thus results in poor electronic conductivity.

In order to improve electrochemical properties of FeF_3, many approaches have been developed, such as adding conductive agents (carbonaceous material) into FeF_3 to form composites by mechanical ball milling, combining with other electro-chemical active materials (MoS_2 [2] or V_2O_5 [3]), etc. Most of the measures focused on coating or adsorption of conductive species on the isolated particles of active materials. For example, Chilin Li group developed a low-temperature ionic-liquid based synthesis method and in-situ synthesized SWNT/$FeF_3 \cdot 0.33\ H_2O$ composite material, which exhibited a remarkable improvement of capacity (e.g., 220 mAh/g at 0.1 C) and good cycle performance (stable capacity around 143 mAh/g at 0.1 C after 30 cycles) in the voltage range of 1.7–4.5 V[4]. FeF_3/MoS_2 composite synthesized by mechanical ball milling showed that the initial discharge capacity was 169.6 mAh g^{-1} and the capacity retention reached 83.1% after 30 cycles[2]. However, almost all of these methods involved alcohol consuming synthesis step, which was considered to be expensive and not suitable for large scale production, and the followed up time consuming ball milling process for the mixing of acetylene black. The complicated multiple steps increased the production cost, raised the risk of exposure to humid air and magnified the possibility of unstable product quality. Furthermore, the synthesis of $FeF_3 \cdot 0.33H_2O$ usually involved the introduction of highly dangerous HF. Otherwise, side reactions and double salts were inevitable.

In this work, we reported a new facile preparation of nanometer-sized $FeF_3 \cdot 0.33H_2O$/acetylene black composite

*Corresponding author. Tel.: +86 574 87600787.
E-mail address: shuimiao@nbu.edu.cn (M. Shui).

0272-8842/$ - see front matter © 2013 Elsevier Ltd and Techna Group S.r.l. All rights reserved.
http://dx.doi.org/10.1016/j.ceramint.2013.09.130

by one step chemico-mechanical ball milling process using $Fe(NO_3)_3$•$9H_2O$ and NH_4F as precursors, which was not only eco-friendly, safe and convenient in the operation, but also easy to realize industrialization.

2. Experimental section

$FeF_3 \cdot 0.33H_2O$/C was synthesized by chemico-mechanical ball milling of $Fe(NO_3)_3$•$9H_2O$ (0.02 mol), NH_4F (0.06 mol), acetylene black (AB, 1.0 g), anhydrous alcohol(1 ml) and polyethylene glycol (PEG 400,1 ml) in an argon-filled and tightly sealed stainless steel vessel for 10 h and desiccation at 120 °C for 24 h in a oven for complete NH_4NO_3 decomposition afterwards.

The crystalline structure was characterized by X-ray diffraction (D8 Advance, Bruker AXS) with Cu Kα radiation. The morphology was observed by a field-emission scanning electron microscope (Hitachi SU-70). FTIR spectrum was recorded on a Shimadzu FTIR-8900 spectrophotometer. Thermal stability of the material was studied by TG/DTA using a Seiko 6300 instrument and the data were collected from room temperature to 800 °C at a heating rate of 10 °C min^{-1} under N_2 protection.

The coin-type cell CR2012 consisting of a metallic lithium foil anode separated by Celgard 2300 polypropylene membrane was fabricated in a glove box filled with high purity argon. The cathode was prepared from a paste by mixing the as-synthesized sample, the conductive acetylene black and the Polyvinylidenefluoride(PVDF) binder with a mass ratio of 4:1:1 in NMP solvent. The paste was coated on the aluminum foil and then dried at 120 °C for 10 h under vacuum before the cell was assembled. The electrolyte was 1 M $LiPF_6$ dissolved in the mixture of EC and DMC (V:V=1:1) solution. Charge/discharge tests were run at current densities of 20 mA g^{-1}, 40 mA g^{-1}, and 60 mA g^{-1}, respectively. Cyclic voltammetry was measured within voltage range 1.5–4.5 V at a scanning rate of 0.1 mV s^{-1}.

3. Results and discussions

The XRD patterns of $FeF_3 \cdot 0.33H_2O$/C and reference $FeF_3 \cdot 0.33H_2O$ (PDF: 76–1262) were shown in Fig. 1 (a). The entire diffraction patterns can be well-indexed to orthorhombic structure with space group Cmcm. No obvious impurities were observed. Acetylene black cannot be discerned for its amorphous character. The weak and broad diffraction peaks of FeF_3/C were indicative of the extremely small crystallite size, which was calculated to be about 25 nm by using the Scherrer equation based on the peak breadth of (002) Bragg reflection on the XRD pattern. The morphological feature and particle size of $FeF_3 \cdot 0.33H_2O$/C composite were also observed from the SEM image. As shown in Fig. 1(b), the dimension of individual particle was estimated to be about 40 nm, which was in good agreement with that obtained by Scherrer equation. Some particles were interconnected with each other to form agglomerates. Usually, small particles with high surface area would benefit the Li^+ transportation.

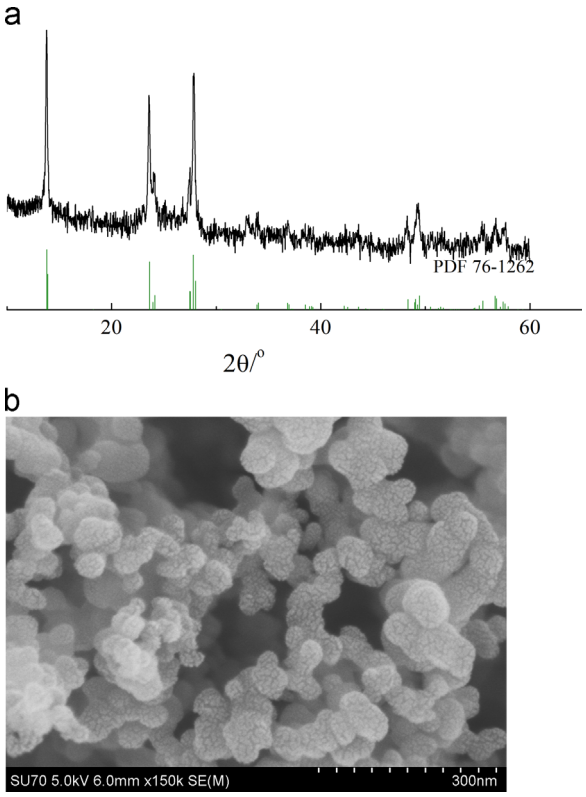

Fig. 1. XRD pattern (a) and SEM imagine (b) of FeF_3/C synthesized via one-step chemico-mechanical ball milling process.

Therefore, higher capacity and better rate capability were anticipated. Evidently, smaller and evenly distributed particles were easy to achieve by this chemico-mechanical method.

The FT-IR spectrum of FeF_3/C composite was illustrated in Fig. 2(a). Due to the Fe–F stretching vibration, a strong band at about 523 cm^{-1} was observed [5]. A strong and broadened absorption band in the region 2850–3450 cm^{-1}, originated from the hydrogen bond association of crystal water, was attributed to –OH stretching vibration. Absorptions at 1631 cm^{-1}, 710 cm^{-1} and 790 cm^{-1} were responsible for H–O–H in-plane and out-plane bending vibrations. The characteristic peaks at 1240 cm^{-1} and 826 cm^{-1} were assigned to acetylene black [5]. Peaks around 1480 cm^{-1} and 1100 cm^{-1} were assigned to $–CH_2$ in-plane bending and C–O–C stretching vibration modes of PEG, respectively.

As can be observed from the TG–DTA curve in Fig. 2(b), the weight loss of $FeF_3 \cdot 0.33H_2O$/C composite happened in three steps. The slight weight loss from room temperature to 240 °C can be attributed to the release of adsorbed water at the surface of $FeF_3 \cdot 0.33H_2O$/C. Then a rapid weight loss about 10.2% detected between 240 °C and 400 °C was attributed to the complete removal of hydration water for $FeF_3 \cdot 0.33H_2O$ and the decomposition of PEG. However, continuous weight loss still occurred from 400 °C to 800 °C, which was much different from the $FeF_3 \cdot 0.33H_2O$ synthesized based on ionic liquid by Li Chilin et al. [6]. This was attributed to the combustion of acetylene black in combination with the partial oxidation of $FeF_3 \cdot 0.33\ H_2O$. According to reference [7], the oxidation of $FeF_3 \cdot 0.33H_2O$ was

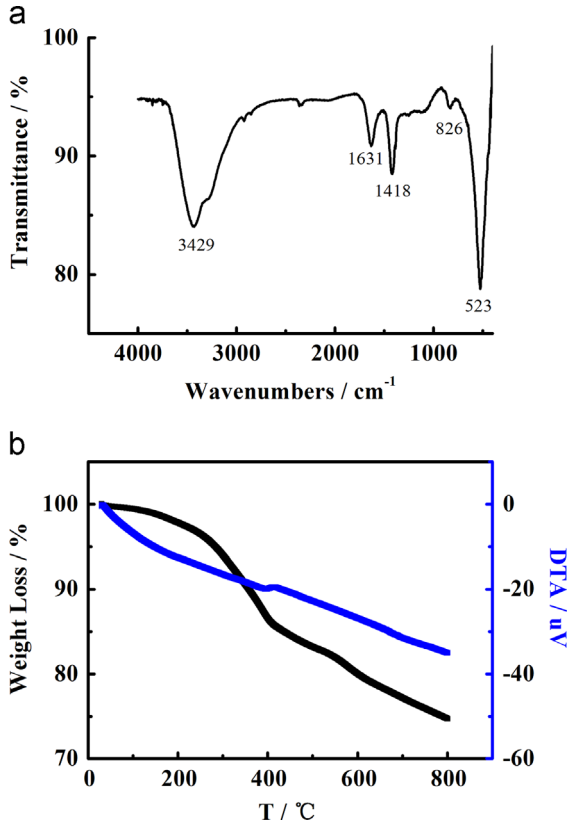

Fig. 2. FT-IR spectrum (a) and TG–DTA chart with a heating rate 10 °C/min under nitrogen protection (b) of FeF_3/C composite.

inevitable when heated above 200 °C. When the temperature further rose up to 400 °C, only iron oxides were left. This would give rise to about 38% weight loss. Here, no apparent oxidation of $FeF_3 \cdot 0.33H_2O$ was observed below 400 °C. This indicated that the acetylene black alleviated the $FeF_3 \cdot 0.33H_2O$ oxidation at high temperature by shielding the material from oxygen corrosion and hence improved the thermal stability of cathode material. Except a small exothermic peak at about 380 °C, corresponding to the removal of hydration water of $FeF_3 \cdot 0.33H_2O$, no obvious thermal effects were observed on the DTA curve.

The charge–discharge processes for $FeF_3 \cdot 0.33H_2O$/C cathodes in the range of 1.8–4.5 V were displayed in Fig. 3a and b. As seen from the voltage profiles (Fig. 3a), the initial discharge capacity of $FeF_3 \cdot 0.33H_2O$/C reached 233.9 mAh g^{-1}, with a corresponding reversible capacity of 186.4 mAh g^{-1}. A lower discharge capacity of 180 mAh g^{-1} delivered in the second cycle and the value of capacity maintained for the tenth cycle showed that the irreversible loss was diminishing upon cycling. Typical sloping discharge plateaus at around 2.7 V were observed, which suggested a solid-solution behavior due to the Li transport [8]. Fig. 3b exhibited the rate performance of $FeF_3 \cdot 0.33H_2O$/C cathodes at various current densities from 20–60 mA g^{-1} and finally back to 20 mA g^{-1}. The cathode material showed good capacity retention and rate capability at increasing discharging rates, indicating that the electrochemical polarization was controlled on a satisfactory level. A reversible capacity of *ca.*157.4 mAh g^{-1} at 20 mA g^{-1} and 117 mAh g^{-1} at 60 mA g^{-1} can be obtained, respectively. Moreover, a capacity of 141.1 mAh g^{-1}

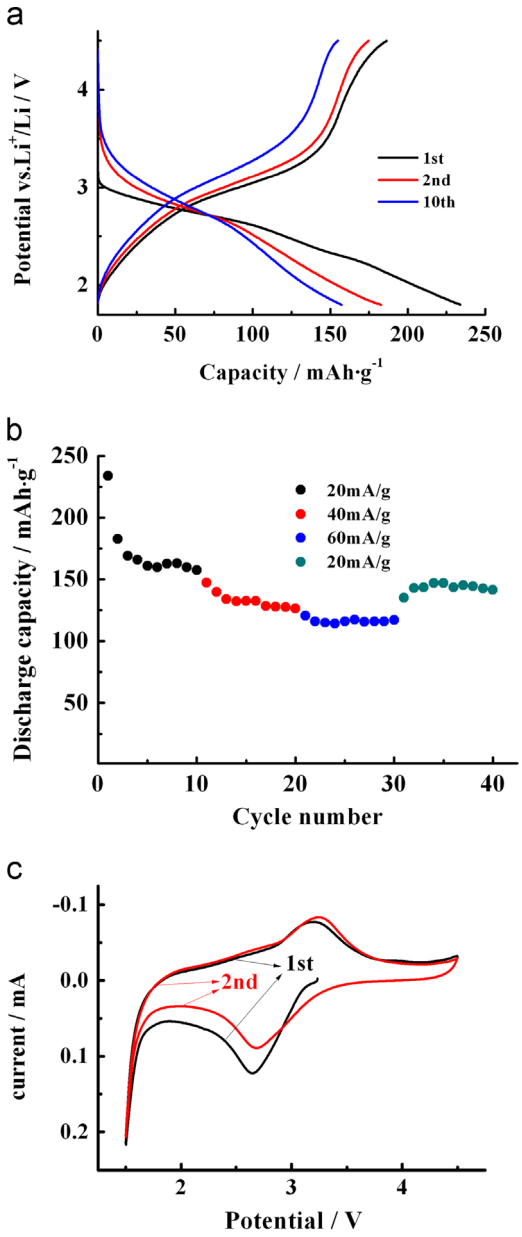

Fig. 3. Charge–discharge profiles at a current density of 20 mA g^{-1} (a), rate performance (b) and cyclic voltammetry at a scan rate of 0.1 mV s^{-1} (c) of FeF_3/C composite.

can be regained when the current density returned to 20 mA g^{-1}. The capacities of FeF_3/C cathodes were comparable to the reported SWNT/$FeF_3 \cdot 0.33H_2O$ composite based on ionic liquid or carbon coated FeF_3 [4,9]. The Cyclic voltammetry for $FeF_3 \cdot 0.33H_2O$/C cathodes was presented in Fig. 3c. For the first scanning loop, it showed a pair of oxidation/reduction peaks located at 3.20 V and 2.65 V, respectively. A reduction peak located at *ca.* 1.5 V was barely distinguishable in the negative scans of FeF_3/C composite, which was supposed to be connected with the conversion reaction $LiFeF_3 + 2Li \rightarrow 3LiF + Fe$ [10]. The potential interval (ΔE) between the oxidation and reduction peak was calculated to be 0.55 V, indicating small polarization and good reversibility in the cycling process. For the second scanning loop, the above mentioned peaks shifted slightly to

higher potentials, which was corresponding to the increase of charge–discharge voltage plateau. These results were in good agreements with the charge–discharge profiles shown in Fig. 3a.

4. Conclusions

In summary, $FeF_3 \cdot 0.33H_2O$/acetylene black composite was synthesized by one step chemico-mechanical ball milling. It showed a noticeable initial discharge capacity of 233.9 mAh g^{-1} and corresponding charge capacity of 186.4 mAh g^{-1}. Good rate capability and cycling performance were also observed. A reversible capacity of *ca*.157.4 mAh g^{-1} at 20 mA g^{-1} and 117 mAh g^{-1} at 60 mA g^{-1} can be obtained, respectively. These results suggested a potential feasibility to use iron fluoride as a high-capacity cathode material by means of further optimization of the synthetic routes.

Acknowledgment

We gratefully acknowledge the support for this work from 973 Fundamental research program from the Ministry of Science and Technology of China (grant number 2010CB635116), NSFC Project 21173190, Educational Commission of Zhejiang Province (grant number Y201017390), Zhejiang Provincial Natural Science Foundation of China Y13B010020, the New Shoot Talents Program of Zhejiang Province (grant number 2013R405069) and K.C.Wong Magna Fund in Ningbo University.

References

[1] M.J. Zhou, L.W. Zhao, S. Okada, J.-I. Yamaki, Thermal characteristics of a FeF_3 cathode via conversion reaction in comparison with $LiFePO_4$, Journal of Power Sources 196 (2011) 8110–8115.

[2] W. Wu, X.Y. Wang, X. Wang, S.Y. Yang, X.M. Liu, Q.Q. Chen, Effects of MoS_2 doping on the electrochemical performance of FeF_3 cathode materials for lithium-ion batteries, Materials Letters 63 (2009) 1788–1790.

[3] W. Wu, Y. Wang, X.Y. Wang, Q.Q. Chen, X. Wang, S.Y. Yang, X. M. Liu, J. Guo, Z.H. Yang, Structure and electrochemical performance of FeF_3/V_2O_5 composite cathode material for lithium-ion battery, Journal of Alloys and Compounds 486 (2009) 93–96.

[4] C.L. Li, L. Gu, J.W. Tong, J. Maier, Carbon nanotube wiring of electrodes for high-rate lithium batteries using an imidazolium-based ionic liquid precursor as dispersant and binder: a case study on iron fluoride nanoparticles, ACS Nano 5 (2011) 2930–2938.

[5] I. Plitz, F. Badway, J. Al-Sharab, A. DuPasquier, F. Cosandey, G. G. Amatucci, Reaction nanocomposites fabricated by solid-state redox conversion structure and electrochemistry of carbon–metal fluoride, Journal of the Electrochemical Society 152 (2005) A307–A315.

[6] C.L. Li, L. Gu, S. Tsukimoto, P. van Aken, J. Maier, Low-temperature ionic-liquid-based synthesis of nanostructured iron-based fluoride cathodes for lithium batteries, Advanced Materials 22 (2010) 3650–3654.

[7] S.-T. Myung, S. Sakurada, H. Yashiro, Y.-K. Sun, Iron trifluoride synthesized via evaporation method and its application to rechargeable lithium batteries, Journal of Power Sources 223 (2013) 1–8.

[8] C.L. Li, L. Gu, J.W. Tong, S. Tsukimoto, J. Maier, A mesoporous iron-based fluoride cathode of tunnel structure for rechargeable lithium batteries, Advanced Functional Materials 21 (2011) 1391–1397.

[9] L. Liu, M. Zhou, X.Y. Wang, Z.H. Yang, F.H. Tian, X.Y. Wang, Synthesis and electrochemical performance of spherical FeF_3/ACMB composite as cathode material for lithium-ion batteries, Journal of Materials Science 47 (2012) 1819–1824.

[10] F. Cosandey, J. Al-Sharab, F. Badway, G.G. Amatucci, P. Stadelmann, EELS spectroscopy of iron fluorides and FeF_x/C nanocomposite electrodes used in Li-ion batteries, Microscopy and Microanalysis 13 (2007) 87–95.